Effect of Initial Texture on Secondary Recrystallization of Grain-Oriented Electrical Steel

I. Iwanaga, H. Masui, J. Harase, K. Iwayama, and N. Takahasi

The effect of initial texture before cold rolling on secondary recrystallization of grain-oriented electrical steel was investigated using thin cast sheets and conventional hot-rolled sheets as initial materials. The main texture component of the surface layer of thin cast sheets is random, while that of the hot-rolled sheets is {110} <001>. It was found that the optimum cold reduction for achieving a strong {110} <001> texture during secondary recrystallization was 95% and 90% for thin cast sheets and hot-rolled sheets, respectively.

Keywords

coincidence boundary, cold rolling reduction ratio, grain growth, microstructure, primary recrystallization, secondary recrystallization, texture, silicon steel

1. Introduction

GRAIN-ORIENTED electrical steel has a sharp {110} <001> texture. This steel is used mainly for transformer cores because of its superior magnetic properties (low core losses and high permeabilities).

Grain-oriented electrical steel is produced by secondary recrystallization. The deviation angle of <100> axis of grains from the rolling direction is smaller than 10° for commercially produced electrical steels.

It has been reported that secondary recrystallization initiates below the surface of primary recrystallized sheets (Ref 1). It is well known that the main texture component of the surface layer of the hot-rolled sheets is {110} <001> (Ref 2). Although many investigations have been made to clarify the mechanism of the development of a sharp {110} <001> texture, it still has not been fully explained why such a sharp {110} <001> texture is produced by secondary recrystallization.

In order to clarify the effect of initial texture before cold rolling on secondary recrystallization, the present study investigated the texture evolution by grain growth using thin cast sheets in which {110} <100> was not the main component of surface texture. It compared the results with those obtained with conventional hot-rolled sheets. Koizumi et al. (Ref 3) studied secondary recrystallization using thin cast sheets in the case of the two-stage cold-rolling method. The present study used a one-stage cold-rolling method to investigate the effect of initial texture on secondary recrystallization.

2. Experimental Procedure

Two types of steels (Specimens A and B) containing MnS and AlN were vacuum melted. The chemical compositions were as follows:

Chemical composition, wt%

Specimen	C	Si	Mn	S	sol Al	N
A	0.06	3.0	0.072	0.029	0.03	0.009
B	0.07	3.1	0.072	0.025	0.03	0.008

Specimen A, thin cast sheet, was cast in 8 mm thickness and was scarfed in 3 mm thickness from both sides. Specimen B, hot-rolled sheet, was cast in 130 mm thickness and was hot rolled at 1350 °C for 90 min to 2.3 mm thickness. They were processed as follows:

- *Hot-band annealing:* 1130 °C for 120 s, water quench at 100 °C
- *Cold rolling:* 0.22, 0.15, 0.12 mm thickness
- *Decarburizing annealing:* 850 °C for 2 min (25% N_2, 75% H_2, dew point 63 °C)
- *Final annealing:* Heating—25% N_2, 75% H_2, 15 °C/h. Soaking—100% H_2, 1200 °C for 20 h

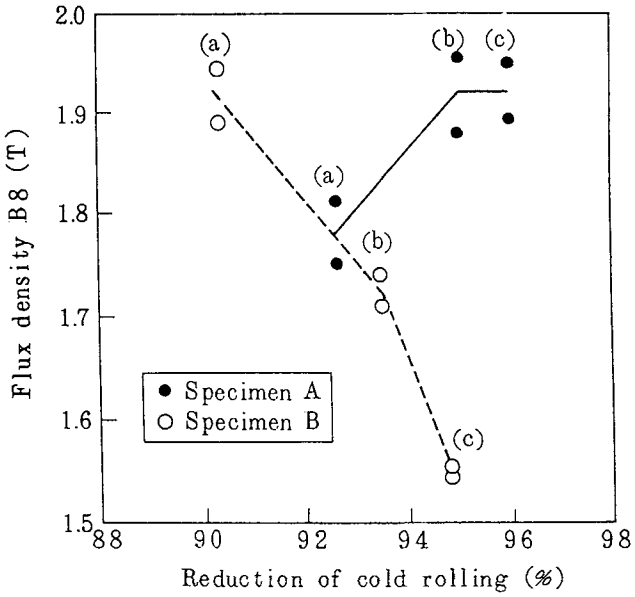

Fig. 1 The effect of cold-rolling reduction on magnetic flux density, B_8

I. Iwanaga, Yawata R & D Laboratory, Nippon Steel Corp., Kitakyushu, Fukuoka, Japan; **H. Masui and J. Harase,** Steel Research Laboratories, Nippon Steel Corp., Futtu, Chiba, Japan; **K. Iwayama,** formerly Nippon Steel Corp., Kitakyushu, Fukuoka, Japan; and **N. Takahasi,** Nippon Steel Corp., Kitakyushu, Fukuoka, Japan

After stress-relief annealing, the magnetic flux density, B_8, was measured in tesla at a magnetizing field of 800 A/m.

Microstructure and macrostructure changes during secondary recrystallization annealing were investigated using an op-

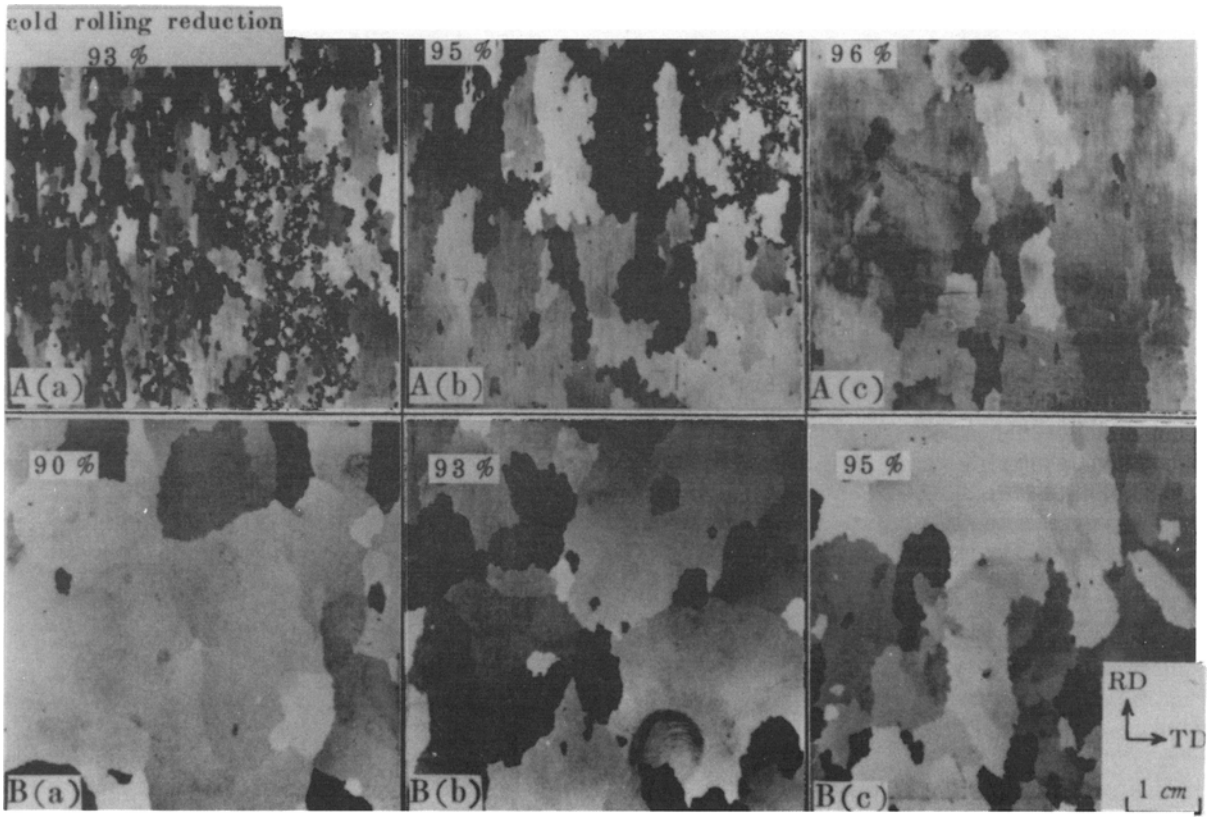

Fig. 2 Macrostructures after final annealing

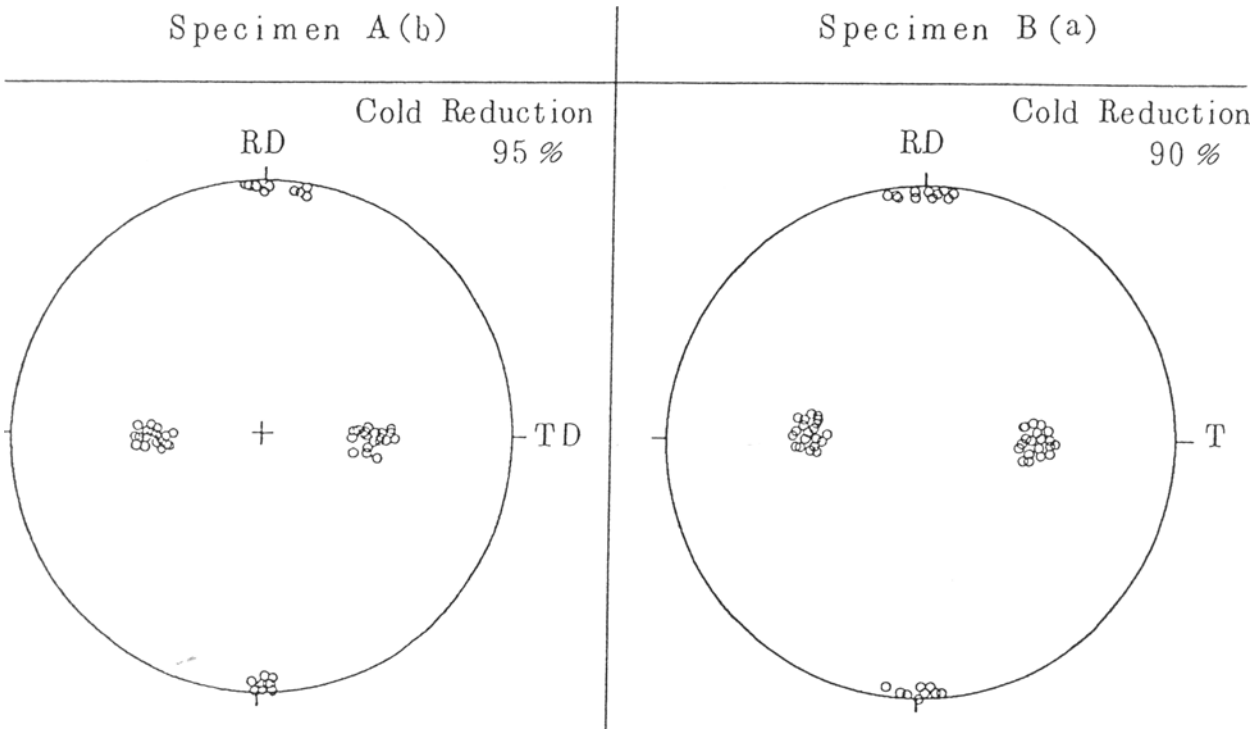

Fig. 3 (200) pole figures of secondary recrystallized specimens

tical microscope and the naked eye, respectively. The grain size of the primary recrystallized specimens was measured using phase contrast image analysis (Ref 4). For the investigation of the primary texture, specimens were extracted from the surface layer that were 70 μm thick, 1/5 the thickness of the primary recrystallized sheet. The complete (200) pole figures were determined by x-ray measurement, and three-dimensional texture analyses were carried out by the vector method (Ref 5). Orientations of the secondary recrystallized grains were determined by the back-reflection Laue diffraction method. The orientation relationships between the secondary recrystallized grains and the matrix primary recrystallized grains were investigated using the Simulation by Hypothetical Nucleus in Generalized form (SHG) method (Ref 6). In the SHG method the intensity of the Σi coincidence orientation in relation to a hypothetical nucleus orientation N is expressed as $I_C\Sigma i$, where the intensities of the orientations analyzed by the vector method are used and Brandon's criterion (Ref 7) is used in the calculation of coincidence orientation.

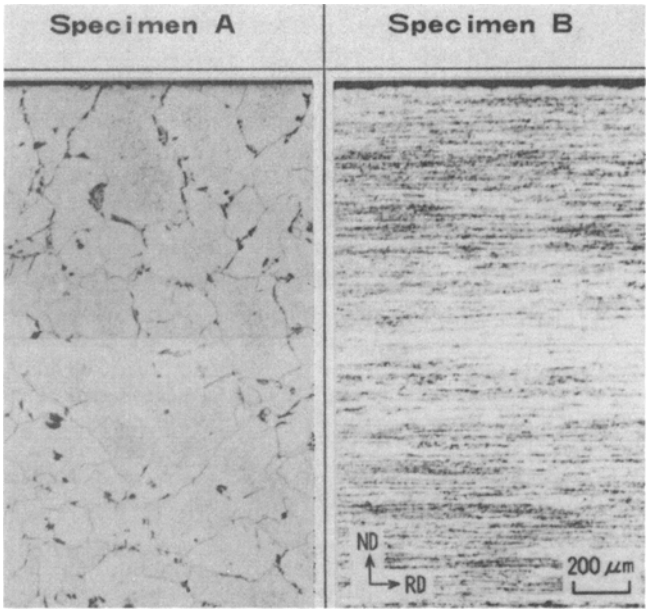

Fig. 4 Microstructures of specimens

3. Experimental Results

Figure 1 shows the magnetic flux density, B_8 of specimens that were stress-relief annealed. The magnetic flux density of specimen A improves with reduction of cold rolling over 90%, but that of specimen B declines steeply.

Figure 2 shows the macrostructure of specimens A and B after final annealing. Fine grains are partly observed in specimen A at the reduction of 93% (Fig. 2A-a), and they decrease in number with increasing reduction until perfect secondary recrystallized grains are achieved at the reduction of 95% (Fig. 2A-b). On the other hand, fine grains are not observed in specimen B at reductions of 90%, 93%, or 95%.

Figure 3 shows (200) pole figures of secondary recrystallized grains. In the case of specimen A at the reduction of 95% (Fig. 3A-b), the number of secondary recrystallized grains with orientations deviated from the ideal {110} <001> was nearly the same as that of specimen B at the reduction of 90% (Fig. 3B-a). This explains the magnetic behavior of specimens A and B as shown in Fig. 1.

Figure 4 shows the microstructures of specimens A and B before cold rolling. Specimen A, which was as-cast, has a very large average grain diameter, 310 μm, and an equiaxed structure, while specimen B has the typical microstructure of hot-rolled sheet. These structures remained the same after annealing.

Figure 5 shows (200) pole figures of the surface layers of specimens A and B before cold rolling. The main texture component of specimen B was {110} <001>, as was generally expected; however, the orientation was nearly random in the case of specimen A.

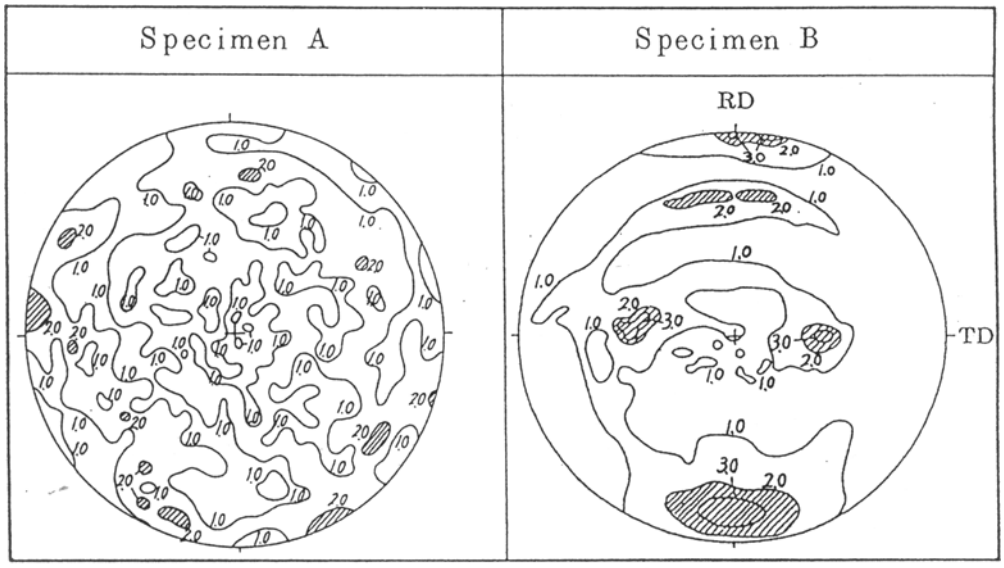

Fig. 5 (200) pole figures of the surface layers of the specimens

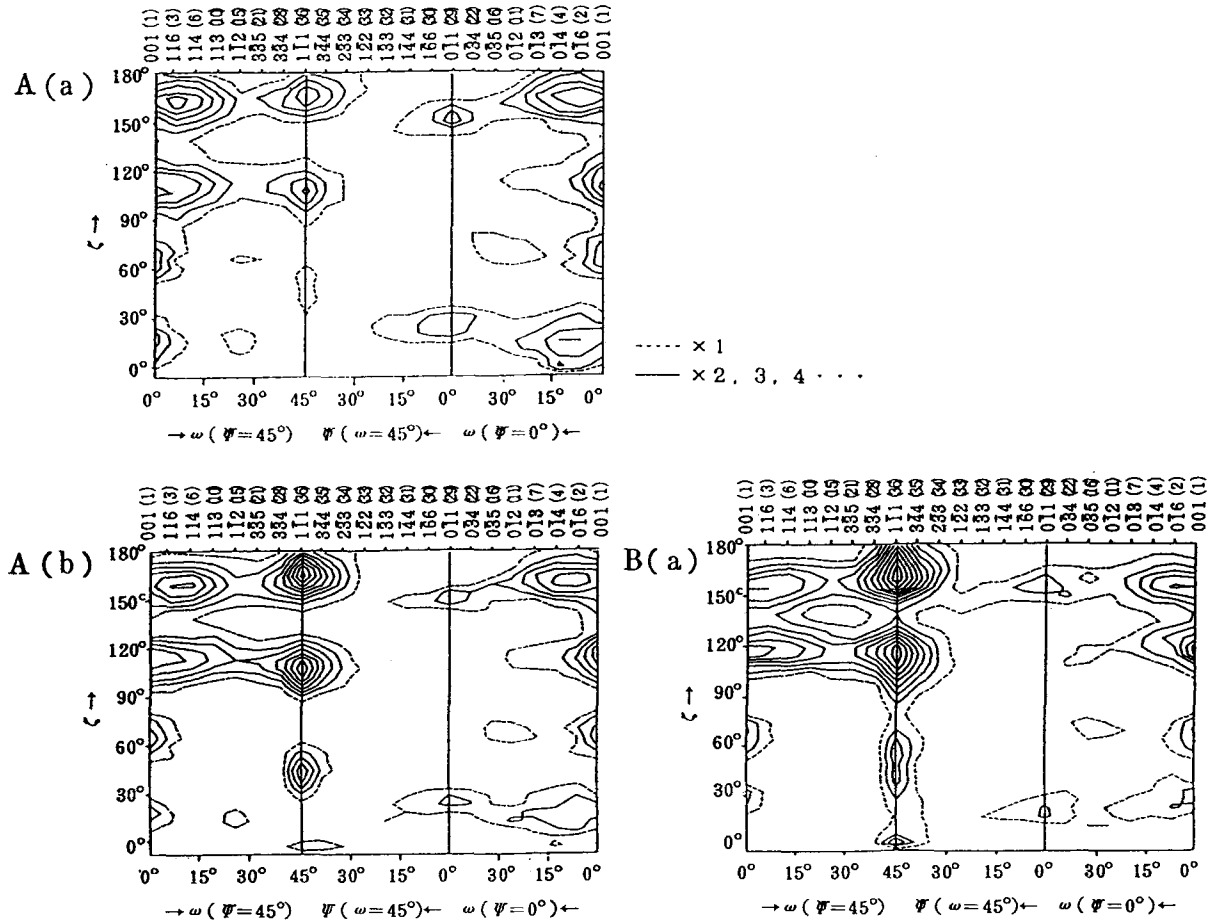

Fig. 6 Three-dimensional orientation distributions converted from (200) pole figures of the surface layers of primary recrystallized specimens. Specimen A: cold-rolling reductions of (a) 93%, (b) 95%. Specimen B: cold-rolling reduction of 90%

Figure 6 shows three-dimensional textures converted from the (200) pole figures of the surface layers of primary recrystallized specimens using the vector method. The main texture components of specimen B were {111} <112>, {411} <148>, and {100} <025>. They remained almost the same with increasing cold-rolling reduction. The component {111} <112> was lower at the reduction of 93% in the case of specimen A. It increased with increasing reduction, and the texture became very similar to that of specimen B.

4. Discussion

It can be seen from Fig. 1 to 3 that perfect secondary recrystallization of a sharp {110} <001> orientation was obtained in the case of specimen A at a higher cold-rolling reduction ratio than in the case of specimen B. This difference of appropriate cold-rolling reduction ratio between specimens A and B is considered to be due mainly to the difference in the initial texture before cold rolling. Figure 6 shows three-dimensional orientation distribution of the primary recrystallized specimens with different cold-rolling reduction ratios. It can be seen that a higher reduction ratio is required for specimen A in order to obtain a texture that is similar to that of specimen B.

Figure 7 shows that the intensity of Σ9 coincidence oriented grains, $I_C\Sigma9$, for {110} <001> increases with increasing cold-rolling reduction. Figure 8 illustrates the relationship between the intensity distribution of $I_C\Sigma9$ and the critical value for the onset of secondary recrystallization. The nucleus orientation having higher $I_C\Sigma9$ than a certain value can be a viable nucleus, and that value is about 25 (Ref 8). The imperfect secondary recrystallization in specimen A with lower cold-rolling reduction can be attributed to the lower $I_C\Sigma9$ value.

It was known that the intensity of {110} <001> orientation decreases with increasing cold-rolling reduction at the primary recrystallized stage (Ref 9) and that the intensity is higher when the initial grain size is large. It was difficult, however, to confirm the intensity of {110} <001> in the primary recrystallized stage by the vector method in the present experiments, because the intensity was too low to be measurable (Fig. 7). The spread of the deviation angle of secondary orientation from 15° to 30° around the normal-direction axis with increasing cold-rolling reduction in specimen B can be due to the lack of intensity in the nucleus of exact {110} <001> orientation. It is considered therefore that the intensity of nucleus orientation as well as $I_C\Sigma9$ is very important for obtaining secondary recrystallization of a sharp {110} <001>. The sharp secondary recrystallization in the case of specimen A at higher reduction might be due to an intensity of nucleus orientation that is higher than the

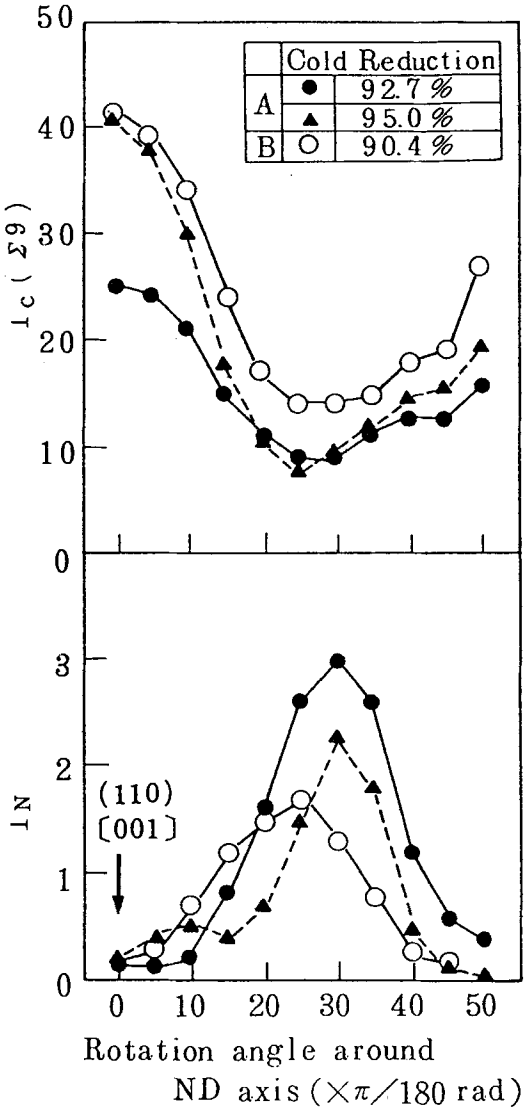

Fig. 7 Distribution of the intensity I_N and I_C (Σ9) of {110} <110> and its rotated orientation around the normal-direction axis of the primary recrystallized specimens

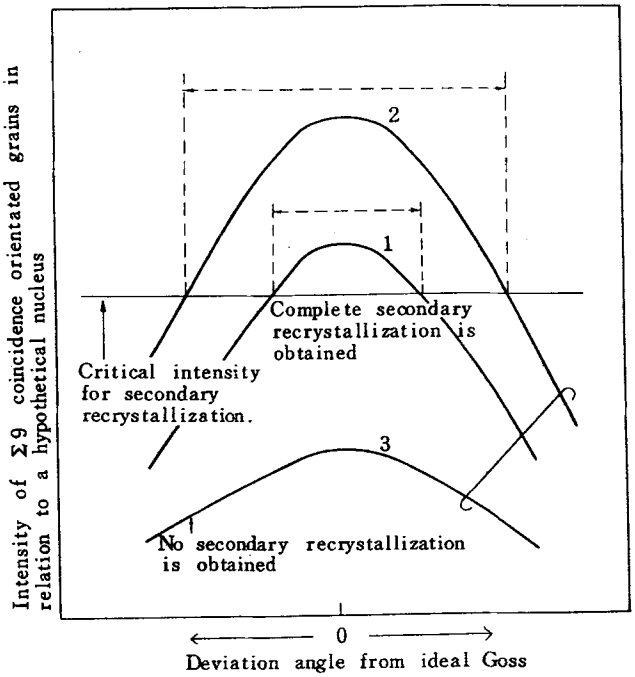

Fig. 8 A schematic diagram explaining the mechanism of obtaining highly oriented {110} <001> secondaries in 3% Si steel. Dashed lines, deviation range of secondaries to be obtained. 1, 2, 3, distribution curves of the intensity of Σ9 coincidence oriented grains

critical value, in addition to the higher $I_C\Sigma9$ value. The presence of {110} <001> at the surface layer before cold rolling is not a prerequisite for the occurrence of sharp secondary recrystallization.

5. Conclusions

The effect of initial texture before cold rolling on secondary recrystallization was investigated using thin cast sheets and conventional hot-rolled sheets as initial materials. The conclusions obtained can be summarized as follows:

- It was found that perfect secondary recrystallization, as seen by achievement of a sharp {110} <001> texture, was obtained at a higher cold-rolling reduction ratio in the thin cast sheets than in conventional hot-rolled sheets.
- Strong {110} <001> texture in thin cast sheets at a high cold-rolling reduction ratio (95 to 96%) is considered to be due to the higher intensity of Σ9 coincidence oriented grains, $I_C\Sigma9$.
- The presence of excess {110} <001> texture in thin cast sheets before cold rolling is not vital for the occurrence of {110} <001> secondary recrystallization because the sheets have no excess {110} <001> texture.

References

1. M. Inokuchi, *Tetsu-to-Hagane*, Vol 70, 1984, p 2033
2. M. Matuo, *Trans. Iron Steel Inst. Jpn.*, Vol 29, 1989, p 809
3. M. Koizumi, T. Kikuchi, and S. Bando, *Tetsu-to-Hagane*, Vol 66, 1980, p 1123
4. Y. Yoshitomi, Y. Matuo, and N. Takahashi, *Materials Forum*, Vol 14, 1990, p 308
5. D. Ruer, A. Vadon, and B. Baro, *Texture of Crystallite Solids*, Vol 3, 1979, p 245
6. R. Shimizu, J. Harase, and D.J. Dingley, *Acta Metall.*, Vol 38, 1990, p 973
7. D.G. Brandon, *Acta Metall.*, Vol 14, 1966, p 1479
8. J. Harase and R. Shimizu, *J. Jpn. Inst. Met.*, Vol 53, 1989, p 745
9. S. Nakashima, K. Takashima, and J. Harase, *Trans. Iron Steel Inst. Jpn.*, Vol 31, 1911, p 1013